A Fiber-Optic System for Measuring Single Excitation–Dual Emission Fluorescence Ratios in Real Time

John F. McCarthy* and Richard L. Magin

Bioacoustics Research Laboratory, Department of Electrical and Computer Engineering, 1406 West Green Street, University of Illinois, Urbana, Illinois 61801

William S. Kisaalita and Patricia J. Slininger

Fermentation Biochemistry Research Unit, National Center for Agricultural Utilization Research, Agricultural Research Service, USDA, 1815 North University Street, Peoria, Illinois 61604

The development and subsequent evaluation of a fiber-optic system for measuring single excitation–dual emission fluorescence ratios in real time is described. The design of the flashlamp excitation source, optics, electronics, and computer software is discussed. The dual emission pH sensitive fluorophore 1,4-dihydroxyphthalonitrile (1,4-DHPN) was used to test the performance of this system. The flexible design of this modular system permits the use of other single excitation–dual emission fluorophores by simply changing the appropriate optical filters. Upon a single 340–380-nm excitation, pH-sensitive emissions were monitored at 488 nm and 434 nm. The ratio of these emissions (488/434) was then computed in real time, for a 2 mM solution of 1,4-DHPN, while the pH was titrated over the range 5–9. The nonlinear, system-dependent, calibration curve of pH versus the ratio of emission wavelengths was empirical fit by a fourth-order polynomial (r^2 = 0.995). Reliable pH measurements in the range 6–8 were obtained using concentrations of 1,4-DHPN as low as 50 μM. The standard deviation of pH measurements using a 1 mM solution of 1,4-DHPN, near neutral pH, was found to be approximately 0.1 pH unit.

1. Introduction

In the last few years there has been increasing interest in the field of fiber-optic chemical sensors. Such sensors offer several advantages over other more conventional sensors including electrical isolation, suitability for use in hazardous environments, potentially small sensor size, and freedom from electrical interference (Narayanaswamy, 1985). Most of the instrumentation used to retrieve data from these sensors have been based on conventional spectrophotometers or spectrofluorometers which have been appropriately modified (Offenbacher, 1986). Since fiber-optic chemical sensors have considerable potential for use in both industrial and biomedical applications, the development of simple, portable, and economical instrumentation suitable for use with these sensors is pressing.

Measurement of radiation at two wavelengths in order to normalize intensity measurements is a well-established technique in analytical chemistry (Jones and Spooncer, 1983) that is well suited for use with fiber- optic technology. A common method is to derive the analyte concentration from the ratio of the radiation measurement at two wavelengths, both of which are equally sensitive to spurious interferences while at the same time being unequally sensitive to the analyte. The principal advantages of this internal referencing technique, over single wavelength intensity measurements, stem from its ability to compensate for measurement errors introduced by variations in source intensity and color temperature, changes in either the amount of indicator or the optical properties of the indicator phase, changes in the "bending loss" of the fiber, connector losses, and drifts in the photodetection and amplification system (Wolfbeis, 1991).

Fiber-optic instrumentation, incorporating an internal reference system, has been reported. A fiber-optic pH measurement system, which uses an incandescent light source, interference filters for wavelength selection, and mechanical modulation, has been developed on the basis of phenol red (Goldstein et al., 1980). A solid-state pH instrument, incorporating light-emitting diode sources and a photodiode detector, has been designed using the indicator bromothymol blue (Guthrie et al., 1988). Both of these systems require dual wavelength excitations and have employed colorimetric indicator dyes.

Until recently, most commercially available fluorophores designed for use in a ratio mode, such as BCECF, fura-2, and HOPSA (Zhujun et al., 1984) also required dual wavelength excitation. Measurements were made with these fluorophores by computing the ratio of fixed wavelength emissions which follow a sequential dual wavelength excitation (Valet et al., 1981). As a consequence, this method has several drawbacks which severely limit both its accuracy and applicability.

Dual wavelength sequential excitation requires high stability in both excitation sources and measurement electronics if the computed ratio is to be independent of systematic error. In addition, fluctuations in the sample characteristics, between excitations, will lead to errors in the computed ratio which can further decrease measurement accuracy. Finally, the usefulness and applicability of this technique are severely restricted by the technical complexities involved in its successful implementation.

At the present time, fluorescence-activated cell sorters and scanning laser microscopes do not possess the capa-

* To whom correspondence should be addressed.

8756-7938/92/3008-0360$03.00/0

bility to alternate excitation wavelengths (Bassnett et al., 1990). Two passes of the same cell or tissue volume through the instrument are required in order to obtain the desired measurement ratio. Since this ratio is computed from measurements made at widely separated points in time, it reflects only the mean value of the actual parameter under investigation. Information regarding the dynamic behavior of the desired parameter is lost as a consequence of the time lag between sequential fluorescence determinations (McCarthy, 1989).

The lack of dynamical information, inherent in the dual wavelength sequential excitation approach, becomes even more problematic when fluorescence ratio based chemical sensors are used to monitor and control chemical processes in real time. In order to design effective process control strategies, the transient dynamic behavior of a chemical process needs to be monitored.

In recent years several new fluorophores, such as 1,4-dihydroxyphthalonitrile (1,4-DHPN), seminaphthorhodafluor (SNARF) (Molecular Probes), and indo-1, have been developed. These preserve the advantages of the ratio technique, while eliminating many of the drawbacks previously associated with dual wavelength sequential excitation spectroscopy. A single, usually broadband, excitation source is used for excitation, and two parallel detection channels are used to achieve simultaneous acquisition of dual wavelength emissions. This feature allows computation of emission ratios in real time, thus preserving the dynamic component of the measurement parameter under investigation. In addition, the use of emission rather than excitation ratios simplifies the design of the instrumentation and algorithms necessary for a wide assortment of applications. To take advantage of the dynamic measurement potential, encompassed within this new class of fluorophores, construction of a specialized fluorescence measurement system was undertaken.

This paper focuses on the development of a fluorescence ratio based fiber-optic measurement system designed for use with dual emission fluorophores. From the design of such a specialized measurement system, a significant reduction in overall system complexity can be obtained. In addition, the use of a single excitation source and a single optical fiber for transmission of both excitation and emission wavelengths greatly simplifies the system design and enhances performance.

Potential applications for such a measurement system are great. These include use in remote fiber fluorometry, where the optical fiber is placed in close proximity to the fluorescent sample. In addition, such systems can be utilized in conjunction with chemically sensing optrodes containing immobilized fluorophore adherent to the tip of an optical fiber.

In the remainder of this paper, the design and operation of a new fluorescence ratio based fiber-optic measurement system is described. The operation of this system was tested using the pH-sensitive dual emission fluorophore 1,4-dihydroxyphthalonitrile (1,4-DHPN) (Molecular Probes, Inc.). However, the flexible design of this modular system permits the use of other single excitation–dual emission fluorophores by simply changing the appropriate optical filters.

2. Instrumentation Design

Instrumentation was designed to enable rapid optical measurement of pH, via the fluorophore 1,4-DHPN, using the dual emission ratio technique. This particular fluorophore disassociates into three distinct species in solution. The predominate species depends on the pH of the solution relative to the pK values for the fluorophore. For 1,4-DHPN, the pK values for the different species were 8.0 ± 0.2 (dianion/monoanion equilibrium) and 5.5 ± 0.3 (monoanion/neutral species equilibrium) (Brown and Porter, 1977). Following a broadband excitation, the peak emission of 1,4-DHPN is shifted to longer wavelengths as the sample pH increases in alkalinity (Kurtz and Balaban, 1985). A difference spectrum (pH 6.0–8.0) shows that the maximal change with pH occurs at wavelengths of approximately 435 nm and 486 nm, respectively. By plotting the ratio of fluorescence emission at two wavelengths (486 nm/435 nm) as a function of pH, an empirical calibration curve was obtained. This empirical curve was adequately fit by a fourth-order polynomial (McCarthy, 1989).

Frequently in spectroscopic work, the short-term stability of the light-source intensity limits measurement speed and accuracy (Scott, 1988). Time-dependent concentration changes may also introduce errors in the measurement of the desired reaction. The dynamic ratio technique, if correctly applied, will provide increases in both measurement speed and accuracy.

2.1. System Design Considerations. A gated integrator approach, using a pulsed source and analog detection, was chosen for simultaneous signal acquisition on each channel. In general, the choice between gated integration (boxcar averaging) and phase-sensitive detection (lock-in detection) is based on the time behavior of the signal (Pease and Wang, 1988). If the signal is fixed in frequency and has a duty cycle greater than or equal to 50%, lock-in detection is the best technique to use. This is because the noise collected during a long gating time can easily swamp the signal. On the other hand, if the signal has a duty cycle less than 50%, such as the pulse from a flashlamp, then a gated integrator technique is best. The advantage of this technique is that it rejects all noise occurring outside the gating interval.

Analog detection was chosen over photon counting on the basis of the expected signal level. At very low light intensities, photon counting works well since the input discriminator tends to reduce front-end noise. At high light intensities, analog detection works better because analog inputs are less prone to saturation. For moderate light levels, such as are inherent in the present application, analog detection was combined with a front-end optimized for low noise operation.

Signal averaging was added to increase the SNR. In its simplest form, signal averaging is just the summation of signals in memory. If the noise is truly random, it will have a mean value of zero and a constant rms value. After n summations, the rms signal amplitude will have increased by n, while the noise will have increased by only $n^{1/2}$. Thus, the SNR at any point is improved by a factor of $n^{1/2}$ (Wright, 1987).

2.2. System Configuration. The block diagram of the measurement system is shown in Figure 1. The four main subsystems [the flashlamp (excitation) source, the optics, the photomultipliers, and the electronics] were each placed in a separate enclosure. Optical connections were made with step index optical fibers (Polymicro Technologies, FHP 500/600/630). These fibers have a synthetic silica core of 500-μm diameter encased within a doped silica cladding containing a thin polyimide outer buffer coating. These materials give a durable low fluorescence optical fiber of approximately 630 μm in total diameter. This fiber has a numerical aperture of 0.22, which results in a full angle acceptance cone of 25.4°, and an attenuation of less than 50 dB/km at a wavelength of 400 nm. These

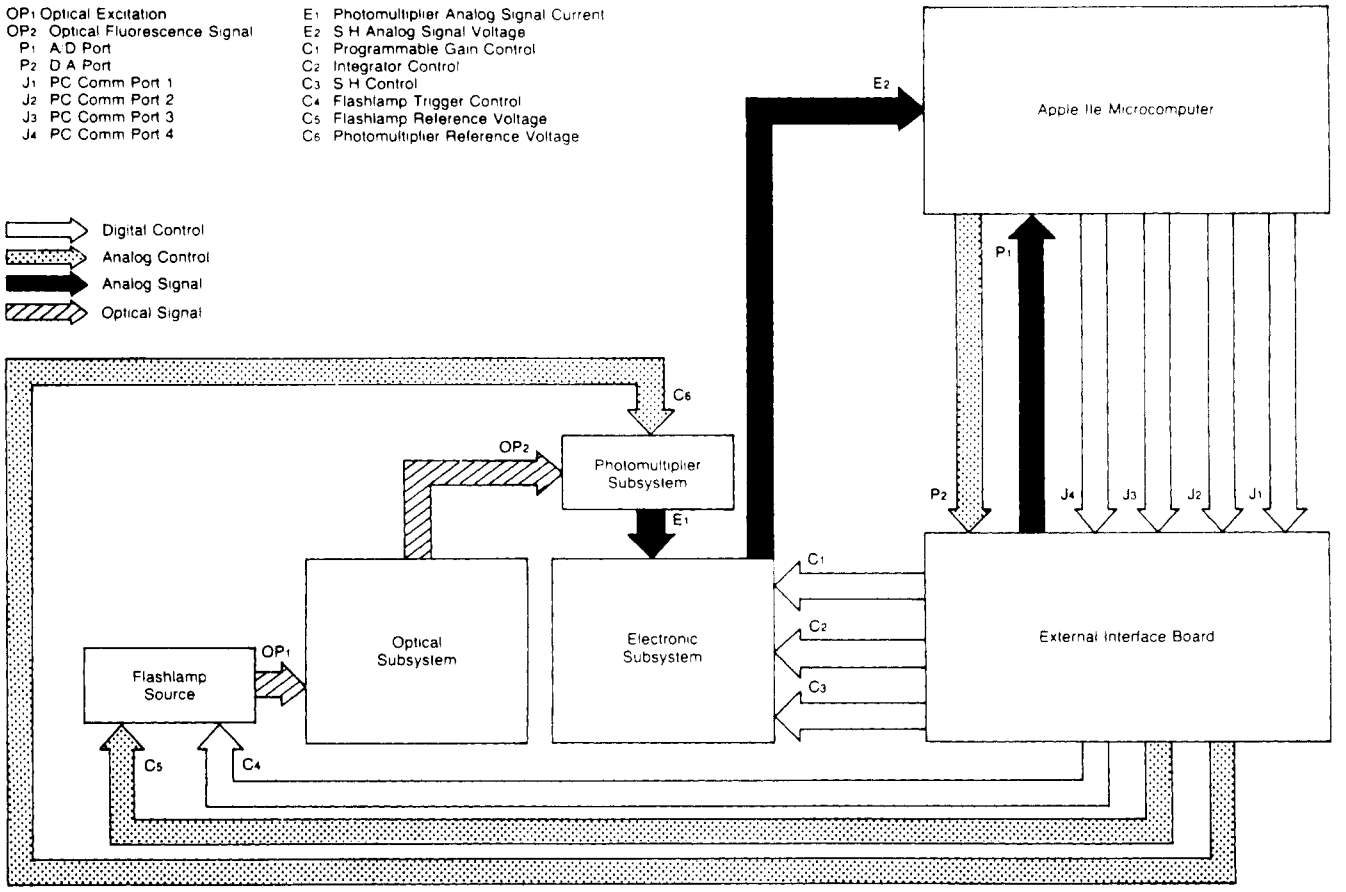

Figure 1. Modular overview of the entire fluorescence ratio based measurement system.

fibers were placed within black Teflon sleeving (Alpha Corp.), in order to ease handling and reduce coupling of stray light into the fiber. After being placed within this sleeving, they were terminated in optical connectors (LFR series) (Amp, Inc.) of the appropriate size. Focusing of the optical beam was accomplished by means of aspheric condensing lenses (Melles Griot, 01 LAG 000). The aspheric surface minimized spherical aberration, allowing a much shorter focal length, for a given diameter, than a spherical lens of equal spherical aberration. This resulted in low *f*-numbers, thus maximizing the collecting area of the lens and concentrating more energy into a fiber located at its focus. Shielded coaxial cables were used to interconnect electrical subsystems. The total system state and parameter settings were controlled by an Apple IIe microcomputer (Apple Computer, Inc.).

2.2.1. Flashlamp. A bulb type Xenon flashlamp (EG&G FX-198), operating at a low repetition rate, was used as a synchronous source of excitation. The output of this lamp was collimated by a parabolic reflector (Melles Griot, 02 RPM 006) and then condensed and shaped by a pair of plano-convex lenses (Melles Griot, 01 LPX 281 and 01 LPX 108). A pulsed flashlamp excitation source was chosen for its ability to deliver higher peak power levels than an equivalent cw-source. In addition, use of a pulsed source eliminates errors introduced by changes in ambient light intensity which might occur outside the pulse interval. The flashlamp excitation spectrum, which has approximately 11% of its optical energy contained within the 300–400-nm range, was filtered by means of a short pass filter (Dell Optics Co.). This filter has an average transmission of 25% form 340 to 380 nm and was blocked to an average optical density of 6 from 430 to 1000 nm. This selected portion of the flashlamp spectrum, chosen to coincide with the excitation spectrum of 1,4-DHPN, was then focused into the proximal end of an optical fiber.

The flashlamp electronics, shown in Figure 2, consisted of the following components: a 24-V at 2.5 A low-voltage supply (Power One); a 300–1500-V programmable high-voltage supply (EG&G PS-350); a flashlamp Lite-Pac trigger transformer (EG&G FYD-506); and two 1-μF energy storage capacitors, connected in parallel and rated at 2 kV. The high voltage was programmed over its full range by means of a 2–10-Vdc external reference supplied by the Apple IIe microcomputer via an 8-bit D/A card (Applied Engineering). Flash duration, measured at one-third peak amplitude, was calculated to be approximately 3.2 ms.

2.2.2. Optics. The optical subsystem, shown in Figure 3, was composed of separate sensor and optical detector modules. Both were similar in overall design and were fabricated out of black Deldrin to decrease the weight of the optical system and to prevent stray reflections from degrading performance. The distal end of the optical fiber, originating in the flashlamp subsystem, connected directly into the sensor module. The sensor module contained a 19-mm diameter dichroic beamsplitter (LPF 1) (Dell Optics Company), mounted at a 45° incidence angle. Excitation wavelengths below 420 nm were reflected and focused into the sensor fiber. Fluorescence wavelengths longer than 430 nm, returning from the sensor tip, were transmitted out of the sensor module by the dichroic device and focused into an output fiber. The broadband fluorescence from this fiber was then focused into the detector module. Within this module a 19-mm diameter achromatic beamsplitter (BS) (Dell Optics Company), mounted at a 45° incidence angle, divided the fluorescence signal into two equal components. Each component was filtered by

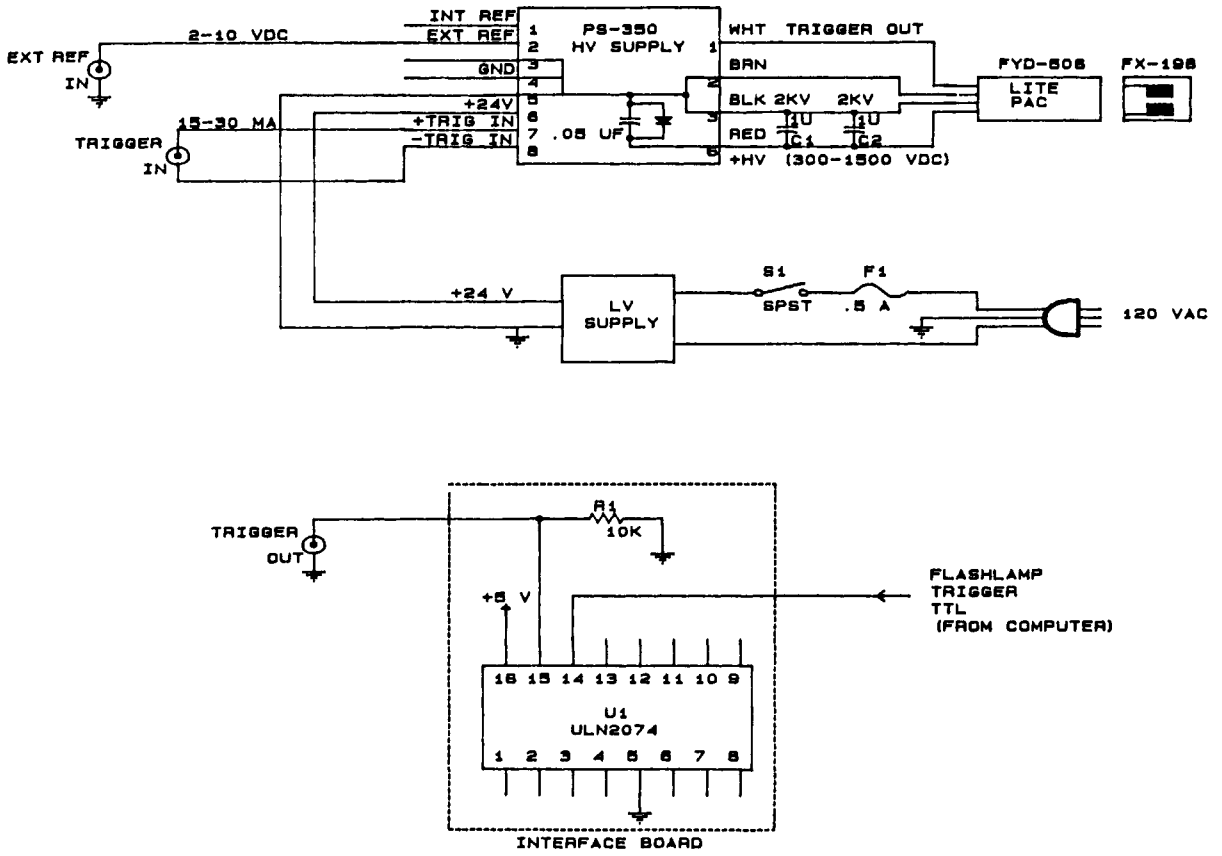

Figure 2. Schematic diagram of the flashlamp electronics.

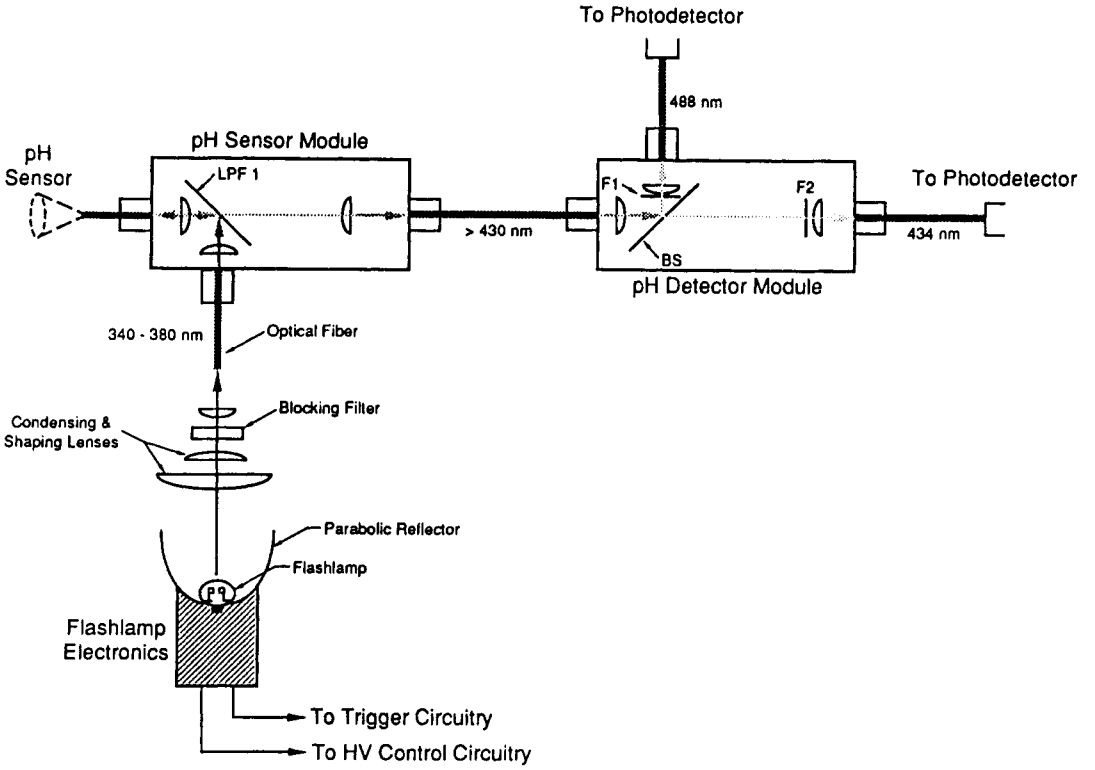

Figure 3. Optical layout of the fluorescence ratio based pH measurement system.

means of a 10-nm band-pass filter, (F1 or F2), centered at either 488 or 434 nm (Dell Optics Company). Each of these 12.5-mm diameter filters has a peak transmission in the passband of approximately 70% and was blocked outside this band to an optical density of 4. The output from these filters was then transmitted out of the detector module and focused into separate optical fibers.

2.2.3. Photomultipliers. Optical fibers carrying 434- and 488-nm emissions were connected to individual photomultiplier tubes. The photomultiplier subsystem, shown schematically in Figure 4, contained the following: two head-on photomultiplier tubes (Hamamatsu, R1463-01) with 13-mm head diameters; two regulated programmable high-voltage supplies (Hamamatsu, C1309-04); two voltage

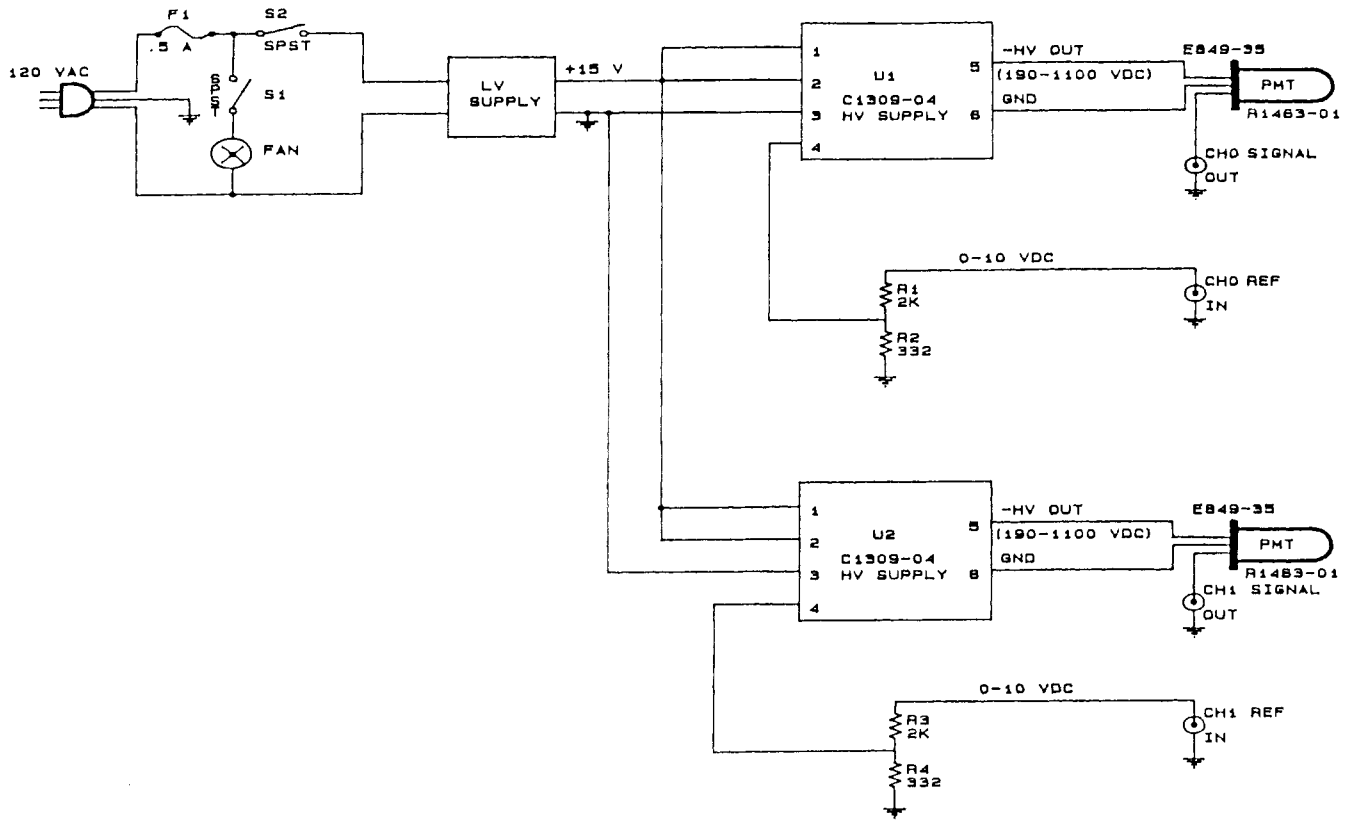

Figure 4. Schematic diagram of the photomultiplier electronics.

divider socket assemblies (Hamamatsu, E849-35); and one 15-V at 1 A low-voltage supply (Power One). These components were housed in an aluminum enclosure to which optical input and electrical input and output connections were made. The gain of the photomultiplier tubes was controlled by the Apple IIe microcomputer, via the programmable high voltage supplies, using the 8-bit D/A card previously discussed. The individual 0–10-V programmable output voltages from the D/A card were divided down, within the photomultiplier enclosure, enabling the photomultiplier electronics to generate high voltages ranging from −190 to −1100 V. This allowed current gains ranging from 4 to over 2×10^6.

2.2.4. Electronics. The electronic subsystem is shown in Figure 5. Two identical electrical channels were available within each module. Timing and digital control signals were generated by the Apple IIe microcomputer through the use of a 6522 parallel interface card (John Bell Engineering, Inc.).

In the main module a low level signal current, from either the internal PIN photodiodes or the photomultipliers, was manually selected via a toggle switch (SW1). These currents were directed into a low noise, low drift (Burr-Brown, OPA101BM), operational amplifier (U1) configured as a current to voltage converter. The gain of this stage was software selectable in four fixed decade steps. Output offsets of this front end amplifier were zeroed via a potentiometer (R5) which formed part of a current injection circuit that was optimized for low drift.

Since high gain amplifier circuits are prone to oscillation when the total phase shift around the feedback loop (including the op amp) reaches 360°, the minimum value of feedback capacitance necessary to stabilize this circuit, while operating at maximum gain, was empirically determined. Since the frequency response of an amplifier is set by the selection of feedback components, a 3-db bandwidth of 16 kHz was directly obtained. For uniformity, the frequency response of this stage was fixed at 16 kHz regardless of the gain setting. A detailed circuit analysis (White, 1987) demonstrates that this bandwidth limitation has no effect on the final integrated output. In other words, although the lowpass filtered signal is reduced in amplitude and dispersed in time, the output from the integrator stage remains unaffected. Thus, the choice of a cutoff frequency represents a compromise between maintaining signal amplitude and reducing the signal dispersion. A large signal amplitude improves the S/N at the output of the first stage (White, 1987), while minimal signal dispersion lessens the necessary integration time, thus improving the S/N at the output of the integrator stage (McCarthy, 1989).

The output of the current to voltage converter stage was coupled directly to a software-controlled Miller integrator stage (U2). The Miller integrator started integration immediately after the flashlamp trigger, using an operator selected integration period. This stage used an operational amplifier (Burr-Brown, 3528AM) selected for its low bias current. A low leakage polystyrene integrating capacitor (C15) was chosen to increase stability. These components enabled use of long integration times without amplifier saturation and also long holding times, such as those used in multiple integrations, without voltage droop.

The output of the integrator stage was coupled to a variable gain stage (U3) built around a standard operational amplifier (LM741C). The configuration of this amplifier was switch selectable (SW2) between inverting and noninverting to accommodate both photodiode and photomultiplier detectors. Four feedback positions were available, each with its own separately adjustable potentiometer. These were selected in tandem with the switchable current to voltage ranges thus, allowing separate calibration of each range as well as the ability to balance the electrical gain between channels. The gain could be

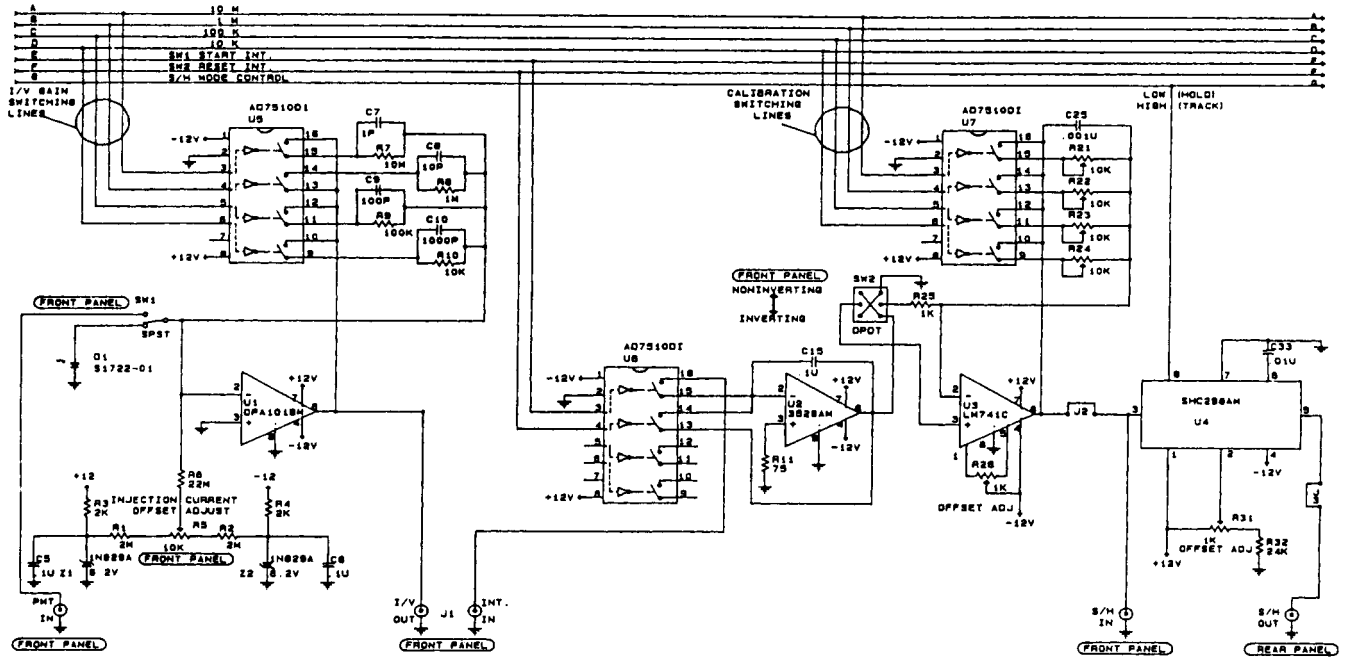

Figure 5. Schematic diagram of a single electronic channel.

varied over approximately one decade. The output of the variable gain stage was coupled to a digitally-controlled sample/hold amplifier (U4) (Burr-Brown, SHC298AM) and routed out of the electronics subsystem via a BNC connector. The dc level from the sample/hold amplifier was multiplexed onto a 16-channel, 12-bit, 25-μs, analog to digital converter card (Applied Engineering) installed within the Apple IIe microcomputer.

2.3. Control Software. The control software runs under the Apple DOS 3.3 operating system on an Apple IIe microcomputer equipped with a Timemaster II H.O. clock card (Applied Engineering). The interactive user interface and data input/output routines were implemented in Applesoft BASIC for convenience. Assembly (6502) language was used to expedite overall system control and data acquisition functions.

The BASIC program was approximately 1000 lines, with calls to assembly language routines which occupied approximately 4 kB of memory. In addition, approximately 2 kB of memory was set aside for data storage and communication between high- and low-level language routines (Ehlert, 1988).

3. Experimental Methods

3.1. Titrations: Fluorescence Ratio versus pH. Simultaneous potentiometric and optical titration were performed using a 2 mM solution of 1,4-DHPN in a 50/50 ethanol/water solvent. This mixed solvent was necessary due to the solubility limitations of 1,4-DHPN at acidic values of pH. This solution was then titrated with a standardized 17.3 ± 0.4 mM NaOH solution (Fritz and Schenk, 1969). The pH during the course of each titration was monitored using a Beckman Model 71 pH meter (Beckman Corporation). The fluorescence signals at 488 and 434 nm, as well as their ratio, were also monitored with a silica optical sensor fiber, as previously described. The system was configured for 8 Hz operation using 1 J of electrical input energy. When the conversion efficiency of the flashlamp source is taken into account, this represents a narrowband optical energy of less than 0.1 μJ at the output end of the excitation fiber (McCarthy, 1989). Integration time was set for 100 μs, with a current/voltage transresistance gain of 1×10^7 and a photomultiplier current gain of 4000 on each channel. Each data point reflects the average of 100 samples, with 2 min of time allowed between data points to ensure adequate mixing of the solution.

3.2. Fluorescence Accuracy and Precision versus Dye Concentration. Sensitivity studies were conducted by varying the concentration of 1,4-DHPN from 1 mM to 5 μM at pH values of 6.0 and 8.0, and from 10 mM to 5 μM at pH 7.0. Various pH phosphate buffers were prepared by mixing stock solutions of 122 mM $Na_2HPO_4 \cdot 7H_2O$ and 122 mM KH_2PO_4 in appropriate combinations. A 10 mM stock solution of 1,4-DHPN was prepared in distilled water and neutralized with NaOH. Instrument settings were essentially the same as those used during titration, except that the photomultiplier current gain was readjusted as necessary. Each data point obtained represents the average of 200 samples.

4. Results and Discussion

The overall performance of the optical ratio based instrument and its suitability for making pH measurements in solution was investigated. This was accomplished using a 1-m length of the previously described optical fiber as a sensor element.

4.1. Titrations: Fluorescence Ratio versus pH. An acid–base titration of 1,4-DHPN was performed. Plots of potentiometrically determined pH and optical fluorescence ratio (488/434), versus titrant volume, were constructed and are shown in Figure 6. The shape of the potentiometrically determined titration curve was typical of that obtained when a weak diprotic acid is titrated with a strong base. The optical fluorescence ratio curve had a very different shape, a continuous smooth curve with no apparent inflection points.

A plot of dual wavelength fluorescence emission intensity versus pH, shown in Figure 7, demonstrates that the fluorescence intensity at 434 nm decreased rapidly as the pH was made more alkaline. Since this wavelength is primarily associated with the monoanionic form of the fluorophore, such a result was not unexpected. However, since a wavelength of 488 nm is primarily associated with the dianionic form of the fluorophore, the fluorescence

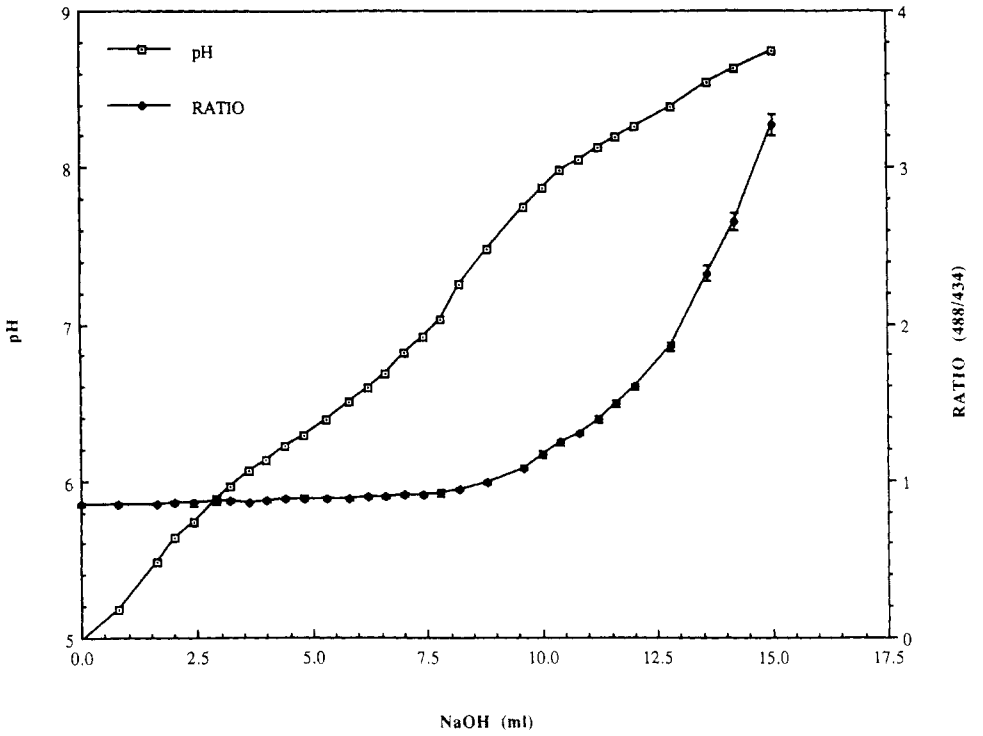

Figure 6. Potentiometric pH and optical fluorescence ratio for a titration of a 2 mM solution of 1,4-DHPN in a 50/50 ethanol/water solvent. The titrant was 17 mM NaOH.

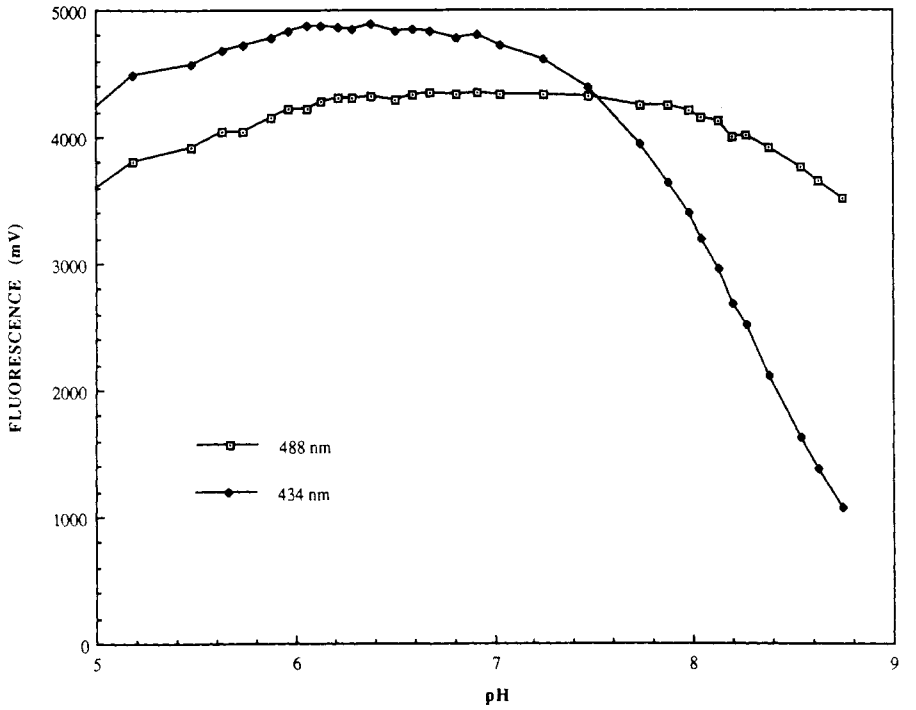

Figure 7. System output at 488 and 434 nm, as a function of pH, during the titration of a 2 mM solution of 1,4-DHPN in a 50/50 ethanol/water solvent.

intensity measured at this wavelength should be expected to increase. The slight decrease actually observed probably results from the dilution of the dianionic species by the added volume of titrant, since such behavior was not seen in studies conducted using a commercial fluorometer and equal volumes of buffered fluorophore (McCarthy, 1989). Alternatively, the broader excitation and emission bandwidths employed in the present system, in conjunction with the complex pH-dependent spectral characteristics of 1,4-DHPN, may result in a reproducible measurement artifact at this wavelength. As long as this artifact is reproducible, it should not impact the accuracy of the pH measurement since the empirically derived instrument calibration curve will automatically account for this aberration.

The fluorescence ratio (488/434) as a function of pH was empirically fit (r^2 = 0.995) by a fourth-order polynomial, over the pH 5–9 range, as shown in Figure 8. This instrumentally generated curve was consistent with the results from previous laboratory studies using this fluorophore (McCarthy, 1989).

4.2. Fluorescence Accuracy and Precision versus Dye Concentration. The relationship between fluorescence intensity and 1,4-DHPN concentration, at pH 7,

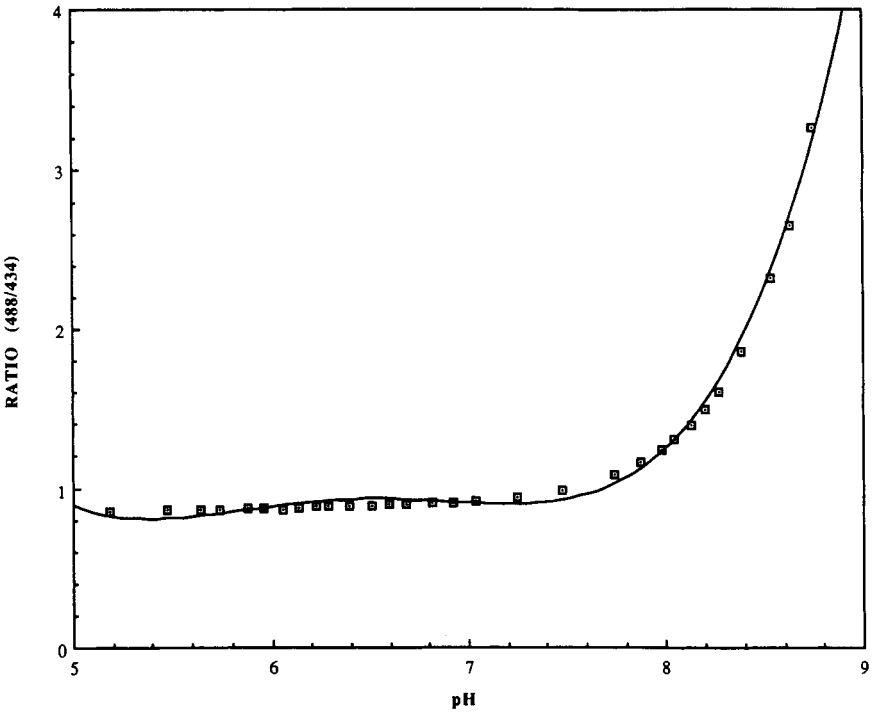

Figure 8. Fluorescence ratio versus pH for a titration of a 2 mM solution of 1,4-DHPN in a 50/50 ethanol/water solvent. A fourth-order polynomial was used to empirically fit the data.

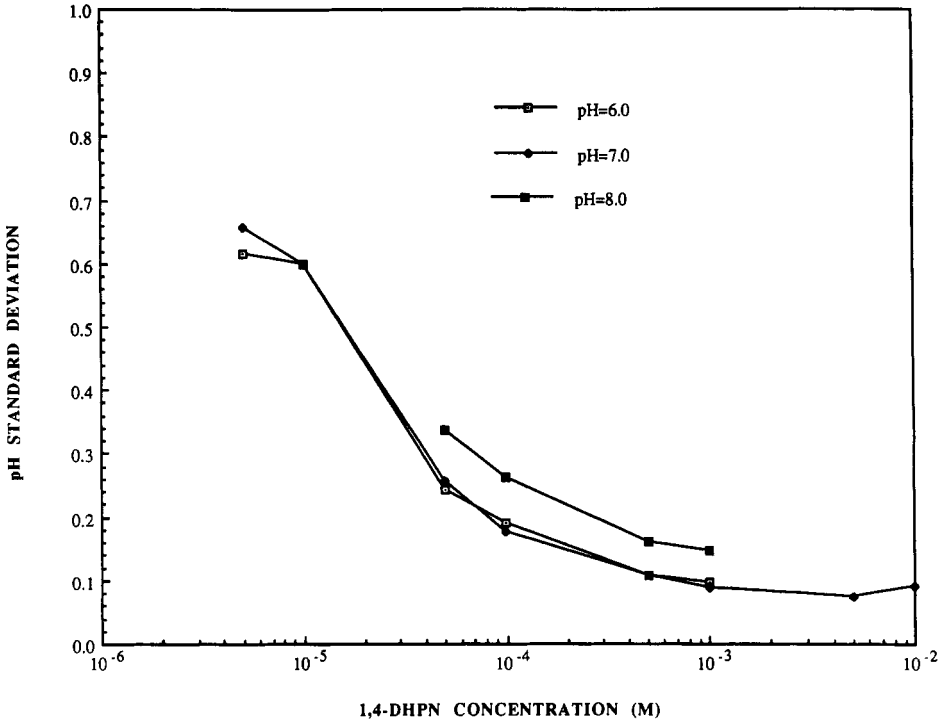

Figure 9. The standard deviation of pH values, as a function 1,4-DHPN concentration at three different values of pH, in phosphate buffer.

was determined. This relationship was found to be an approximately linear function of 1,4-DHPN at concentrations ranging from 10 μM to 1 mM. However, for all concentrations of fluorophore used in this experiment, the fluorescence ratio (488/434) was independent of concentration. The standard deviation of the ratio increased as the fluorophore solution became more dilute. For any concentration of 1,4-DHPN, the measurement error increased with alkalinity, as a consequence of the decreasing level of 434-nm fluorescence. As the level of 434-nm fluorescence approaches zero, the fluorescence ratio (488/434) becomes extremely sensitive to small changes in the denominator. Thus, system noise tends to greatly impact the accuracy of measurements made in alkaline solutions.

The present measurement system was configured for operation with an electrical input energy of 1 J, a flash rate of 8 Hz, an integration time of 100 μs, and a current/voltage transresistance gain of 1×10^7. Using these parameter settings, a 1 mM solution of 1,4-DHPN was required to obtain pH measurements with standard deviations less than 0.1 pH unit. This result was obtained at neutral pH, when 200 samples were averaged. Given this set of operating parameters, the above measurement

precision was close to the maximum obtainable with this system regardless of concentration. A plot of pH errors for other concentrations and pH values was obtained and is shown in Figure 9.

5. Conclusions

A fluorescence emission ratio based fiber-optic measurement instrument was developed and evaluated using the pH-sensitive dual emission fluorophore 1,4-DHPN. This instrument was found to be capable of measuring the pH of near neutral solutions of 1 mM fluorophore with a standard deviation of better than ±0.1 pH unit.

Although this instrument was demonstrated in conjunction with a specific dual emission pH-sensitive fluorophore, it can easily be adapted to work with different dual emission fluorophores by simply changing the optical filters. This would allow sensing of any chemical species detectable by dual emission fluorescence ratios.

As newer dual emission fluorophores become available, new optrodes will be designed and fabricated to take advantage of their unique properties. As a consequence, simple, portable, and economical instrumentation, such as the system described in this paper, should find increasing utility in numerous and diverse areas of scientific investigation.

The ability of this instrument to perform real time ratio measurements in a practical dynamic environment is the subject of a related paper (Kisaalita et al., 1991).

Supplementary Material Available: Applesoft BASIC Initialization and Control Program Listing and 6502 Assembly Control Program Listing (65 pages). Ordering information is given on any current masthead page.

Literature Cited

Bassnett, S.; et al. Intracellular pH Measurement Using Single Excitation-Dual Emission Fluorescence Ratios. *Am. J. Physiol.* **1990**, *258*, C171–C178.

Brown, R. G.; Porter, G. Effect of pH on the Emission and Absorption Characteristics of 2,3-Dicyano-*p*-hydroquinone. *J. Chem. Soc., Faraday Trans. I* **1977**, *73*, 1281–1285.

Ehlert, K. S. *System Design and Development for Control, Acquisition, and Analysis of Signals from Fiber Optic Sensors.* M.S. Thesis, University of Illinois, 1988.

Fritz, J. S.; Schenk, G. H. *Quantitative Analytical Chemistry*; Allyn and Bacon, Inc.: Boston, 1969.

Goldstein, S. R.; et al. A Miniature Fiber Optic pH Sensor for Physiological Use. *J. Biomech. Eng.* **1980**, *102*, 141–146.

Guthrie, A. J.; et al. Solid-State Instrumentation For Use With Optical-Fibre Chemical-Sensors. *Talanta* **1988**, *35* (2), 157–159.

Jones, J. E.; Spooncer, R. C. Two-Wavelength Referencing of an Optical Fibre Intensity-Modulated Sensor. *J. Phys. E.* **1983**, *16*, 1124–1126.

Kisaalita, W. S.; et al. Application of Fiber-Optic Fluorescence Measurements to On-Line pH Monitoring of a Pseudomonad Fermentation Process. *Biotechnol. Prog.* **1991**, *7*, 564–569.

Kurtz, I.; Balaban, R. S. Fluorescence Emission Spectroscopy of 1,4-Dihydroxyphthalonitrile: A Method for Determining Intracellular pH in Cultured Cells. *Biophys. J.* **1985**, *48*, 499–508.

McCarthy, J. F. *Development and Evaluation of a Fluorescence Emission Ratio Based Fiber Optic pH Measurement System for Use in Monitoring Changes in Tumor pH During Clinical Hyperthermia.* Ph.D. Thesis, University of Illinois, 1989.

Narayanaswamy, R. Fibre Optics for Chemical Sensing. *Anal. Proc.* **1985**, *22*, 204–206.

Offenbacher, H. Fluorescence Optical Sensors for Continuous Determination of Near-Neutral pH Values. *Sens. Actuators* **1986**, *9*, 73–84.

Pease, J. S.; Wang, J. C. Gated Photon Counting Can Improve Optical Measurements. *Laser Focus* **1988**, *24* (2), 102–105.

Scott, J. Lock-Ins Handle Ratioed Optics Measurements. *Laser Focus* **1988**, *24* (6), 104–112.

Valet, G.; et al. Fast Intracellular pH Determination in Single Cells by Flow-Cytometry. *Naturwissenschaften* **1981**, *68*, 265–266.

White, T. G. *Design and Noise Analysis of an Operational Amplifier–Photodiode Pair for Use in Fiber Optic Sensors.* M.S. Thesis, University of Illinois, 1987.

Wolfbeis, O. S. *Fiber Optic Chemical Sensors and Biosensors*; CRC Press: Boca Raton, FL, 1991, Vol. I.

Wright, J. C. You Can Find Treasure Hidden in the Trash. *Res. Dev.* **1987**, *29* (2), 140–143.

Zhujun, Z. and Seitz, R. A. Fluorescence Sensor for Quantifying pH in the Range from 6.5 to 8.5. *Anal. Chim. Acta* **1984**, *160*, 47–55.

Accepted April 9, 1992.

Registry No. 1,4-DHPN, 4733-50-0.